

Journal of Materials Chemistry A

Accepted Manuscript



This is an *Accepted Manuscript*, which has been through the Royal Society of Chemistry peer review process and has been accepted for publication.

Accepted Manuscripts are published online shortly after acceptance, before technical editing, formatting and proof reading. Using this free service, authors can make their results available to the community, in citable form, before we publish the edited article. We will replace this *Accepted Manuscript* with the edited and formatted *Advance Article* as soon as it is available.

You can find more information about *Accepted Manuscripts* in the [Information for Authors](#).

Please note that technical editing may introduce minor changes to the text and/or graphics, which may alter content. The journal's standard [Terms & Conditions](#) and the [Ethical guidelines](#) still apply. In no event shall the Royal Society of Chemistry be held responsible for any errors or omissions in this *Accepted Manuscript* or any consequences arising from the use of any information it contains.

Crystal Structure, Defect Chemistry and Oxygen Ion Transport of the Ferroelectric Perovskite, $\text{Na}_{0.5}\text{Bi}_{0.5}\text{TiO}_3$: Insights from First-Principles Calculations

James A. Dawson^{a*}, Hungru Chen^b and Isao Tanaka^a

^a*Department of Materials Science and Engineering, Kyoto University, Sakyo, Kyoto, 606-8501, Japan*

^b*Environmental Remediation Materials Unit, National Institute for Materials Sciences, Ibaraki, 305-0044, Japan*

ABSTRACT

Recent experimental studies have shown how A-site nonstoichiometry in $\text{Na}_{0.5}\text{Bi}_{0.5}\text{TiO}_3$ (NBT) can dramatically alter its electrical properties and conduction mechanisms. In nominal NBT and Bi-deficient $\text{NBi}_{0.49}\text{T}$, electrical conductivity primarily comes from oxygen ion conduction and not electronic conduction. This is contrary to the behaviour of traditional titanates and could potentially give NBT a role in the design of new intermediate-temperature solid oxide fuel cells (SOFCs). In this study, we use density functional theory (DFT) with the Hubbard U correction to investigate the much debated local structure and defect chemistry of NBT, with the primary focus on oxygen vacancy formation and oxygen ion transport. We confirm significant cation and oxygen displacement in both the Cc and $R3c$ structures. Small ordering energies confirm an essentially random distribution of A-site ions. Oxygen vacancies are shown to preferentially form in the vicinity of Bi ions, confirming that weak Bi-O bonds do indeed promote oxygen ion migration. Nudged elastic band (NEB) calculations predict oxygen migration energies that are in excellent agreement with experiment. Oxygen ion migration to Bi-rich chemical environments is generally shown to be unfavourable, while migration to Na-rich chemical environments produces lower migration energies. Our calculations confirm many of the assumptions recently reported in experimental studies and provide a far greater understanding into the unique and complex defect chemistry of NBT than is currently available.

Keywords: *oxygen ion conductors, NBT, ferroelectric, perovskite, DFT*

Electronic mail: doson5888@gmail.com

Telephone number: +81-75-753-5435

1. Introduction

As a result of its unusual electrical properties and its potential ability to replace lead zirconate titanate (PZT) as a lead-free piezoelectric material¹⁻³, $\text{Na}_{0.5}\text{Bi}_{0.5}\text{TiO}_3$ (NBT) has received significant attention in recent years. In addition to being a leading candidate for the replacement of PZT in electromechanical actuators, sensors and transducers, NBT shows strong ferroelectric properties^{4,5} and is often used in solid solutions with other ferroelectric materials like BaTiO_3 and $\text{K}_{1-x}\text{Na}_x\text{NbO}_3$ for both piezoelectric and capacitor applications⁶⁻¹⁰. Recent studies have also reported on the potential application of NBT-based materials in intermediate-temperature solid oxide fuel cells (SOFCs) on the basis of their unusual oxygen ion conduction properties^{11,12}.

Despite being discovered in 1960¹³, much controversy still exists over the complex local structure of NBT including chemical Bi/Na ordering, octahedral rotations and cation displacements¹⁴. The room temperature rhombohedral structure of NBT was originally confirmed as space group $R3c$ by neutron diffraction studies¹⁵. However, recent high resolution synchrotron powder X-ray diffraction data suggests that it is actually a monoclinic structure with space group Cc ¹⁶. Further complication arises from the fact that the average structure discussed above is different from the complex local structure determined from X-ray and neutron total scattering experiments and pair distribution function (PDF) analysis^{12,17,18}. The difference between local and average structure is primarily a result of the different displacements of Na and Bi ions¹⁷ and in-phase and out-of-phase octahedral tilting¹⁴.

The chemical ordering of Bi and Na in NBT is a much debated topic. Transmission electron microscopy has been recently used to confirm a random distribution of Bi and Na with no A-site ordering¹⁴. Alternatively, Kreisel *et al.*¹⁹ used X-ray diffuse scattering experiments to show chemical short-range ordering which could be responsible for

segregation planes with correlated cation displacements. Density functional theory (DFT) calculations have suggested that local chemical ordering can exist because of the hybridization of Bi $6sp$ and O $2p$ states which leads to stereochemically active Bi³⁺ lone pairs and stable structures with high Bi concentrations in the (001) planes²⁰. Such local ordering is, however, only likely to occur at short-range because of the small ordering energies between structures. We direct the reader to ref 14 for a more detailed discussion of Bi and Na distribution in this material.

In addition to its highly complex crystal structure, NBT also possesses a wealth of distinctive electrical properties^{4-6,21-23}. In the past few years, numerous studies on the dramatic effect of A-site stoichiometry on these electrical properties have been completed. Hiruma *et al.*⁵ reported that small changes in A-site stoichiometry can alter the dc resistivity of NBT by 3 orders of magnitude and dramatically change the electrical properties. They found that compositions with Na excess or Bi deficiency lower dc resistivity and the piezoelectric (d_{33}) coefficient, while increasing the depolarization temperature (T_d). Alternatively, Na deficiency or Bi excess in samples enhances the dc resistivity and d_{33} , while reducing T_d ^{5,21}. A more recent study investigated the effect of A-site stoichiometry on the ferroelectric properties of NBT²⁴. They discovered that changes to the A-site stoichiometry decreased the spontaneous ferroelastic strain of the unit cell and that Bi deficient/Na excess compositions displayed significantly inferior ferroelectric properties and were unable to be poled to induce piezoelectric coefficients. Such studies clearly illustrate the importance in controlling the A-site stoichiometry as it can have a drastic effect on the structural and electrical properties of NBT.

Furthermore, A-site stoichiometry in can also influence the levels of conduction and indeed the actual conduction mechanisms in NBT. Two recent studies in particular have illustrated how control of A-site stoichiometry can be used to produce high levels of oxygen ion

conduction in NBT, giving it potential application in SOFCs^{11,12}. This is despite the fact that electrical conductivity in titanates usually comes from electronic conduction^{11,12}. Li *et al.*¹¹ used a combination of experimental techniques including ¹⁸O tracer diffusion and impedance spectroscopy to determine that high leakage conductivity in NBT, a common problem in piezo- and ferroelectric applications, is actually the result of oxygen ion conduction due to Bi deficiency and oxygen vacancies induced during materials processing. It was found that while NBT samples with excess Bi are insulating, A-site stoichiometric and Bi deficient samples are conducting. The reason for this unique behaviour is believed to be a result of highly polarized Bi ions and weak Bi-O bonds which are responsible for the softness of the polar NBT lattice, which makes it a good structure for oxygen ion conduction, in addition to piezo- and ferroelectricity. Mg-doping at the Ti-site was also considered to increase the oxygen vacancy concentration and thus the ionic conductivity. This proved successful and not only increased the ionic conductivity, but also improved the electrolyte stability in reducing atmospheres and lowered the sintering temperature.

Here we report the first comprehensive computational study of oxygen vacancies and transport in NBT. Despite the obvious importance and wide ranging applications of this material, the number of theoretical studies focused on it in the literature is severely limited. We begin by assessing the local structure and calculating the energetics of A-site ordering for both the *Cc* and *R3c* structures. We then proceed to calculate the energetics of oxygen vacancy formation and migration in these same structures. All oxygen sites are considered and several migration pathways are constructed for each NBT configuration to ensure that the consequences of the many different local structural and chemical environments are fully assessed.

2. Methodology

DFT+ U calculations in this work were performed using the Vienna *Ab initio* simulation package (VASP)²⁵ with the generalized gradient approximation (GGA) according to Perdew, Burke and Ernzerhof²⁶ and the projector augmented-wave method²⁷. For greater accuracy, the semi core s electrons of O, the semi core p electrons of Na and Ti and the semi core d electrons of Bi are treated as valence electrons for all calculations. The chosen value of the Dudarev correction²⁸ for the Ti ion was $U = 4.2$ eV. This value was obtained by fitting to experimental data the splitting between occupied and unoccupied Ti d states for oxygen vacancy states at the (110) surface of rutile TiO₂^{29,30}. A plane wave cutoff energy of 600 eV was applied for all calculations. A Γ -point centred $2 \times 2 \times 2$ k -point mesh was used for Brillouin zone integration. The structural relaxations were completed when the residual force of each atom was less than 0.01 eV/Å. Careful checks were also performed to ensure adequate convergence with respect to the applied basis set and the k -point mesh. The total energy of the supercells was found to converge reasonably rapidly with planewave cut-off energy and our value of 600 eV was found to be more than sufficient. Similarly good total energy convergence was also observed for our chosen k -point grid.

All calculations were completed using supercells each consisting of 120 ions. For the Cc structure, a supercell of $1 \times 3 \times 2$ unit cells was used and for the $R3c$ structure, a supercell of $2 \times 2 \times 1$ unit cells was used. Comparison between the two structures is made easier through the use of supercells with the same number of ions. One oxygen vacancy in either supercell is equivalent to an oxygen deficiency of 1.4 %. All of the calculations in this work consider the A-site of NBT to be fully stoichiometric i.e. Na_{0.5}Bi_{0.5}TiO₃.

Oxygen migration in perovskites occurs through via a vacancy hopping mechanism. The oxygen ion travels through the bottleneck of the “critical triangle” formed between one B-site

cation and two A-site cations³¹ and its pathway is often slightly curved away from the B-site cation³². Minimum energy path calculations between two optimized configurations each with an oxygen vacancy were completed using the NEB method where the migration path is divided into a number of equidistant configurations known as images. For all the migration calculations in this work, seven images are used. The images of the migration path are connected with springs and their positions optimized. In the NEB method, optimization uses the spring force along the direction of the migration path (to prevent the images from sinking into the minima) in addition to the true force along the direction perpendicular to the migration path (to ensure the lowest energy path is obtained).

3. Results and Discussion

3.1. A-Site Ordering and Relative Stability of the *Cc* and *R3c* Structures

In order to find the lowest energy NBT configurations for the calculation of oxygen vacancy formation and migration, we calculated the total energies of several possible A-site orderings in both the *Cc* and *R3c* structures. Recent experiments have shown that A-site ordering is completely random in NBT¹⁴, whereas simulations have suggested that ordering at short-range is possible²⁰. In order to truly assess A-site ordering in these two structures, we would require larger cells and we would have to consider many thousands of configurations. As the primary focus of this work is the defect chemistry of oxygen vacancies, this is beyond the scope of this work. Therefore, we only consider three simple types of layered ordering; rock salt (111), (110) and (001). Several other types of ordering have been considered previously, but were found to be less energetically stable than the (001) layer ordering²⁰.

Fig. 1 shows the three Cc configurations considered. As reported by experiment¹⁷, we observe significant displacement of the A-site ions in all Cc and $R3c$ configurations tested. Table 1 displays the calculated structural parameters and relative stabilities of the three Cc unit cell configurations. All of the configurations reproduce the experimental lattice parameter well considering the typical overestimation of lattice parameters by the GGA functional. Of the three structures, the lowest energy is found for the (001) layered ordering, however it must be noted that the relative stabilities of all the configurations are very similar meaning that the thermal energy will dominate. Similar results were found for the cubic structure of NBT with A-site ordering in the $\langle 001 \rangle$ lattice planes found to be favoured²⁰. Although, the difference between the energy of the most and least stable configurations found in their study (> 0.2 eV) was significantly higher than the value in this study. The existence of strong rock salt ordering ((111) layered) has been considered in NBT³³, however in agreement with other computational studies^{20,34}, we can rule this possibility out as it is the least stable of the three configurations considered. The calculated small ordering energies do suggest that no one particular ordering is significantly dominant over the others, thus reinforcing the argument that a random distribution of A-site ions exists in NBT.

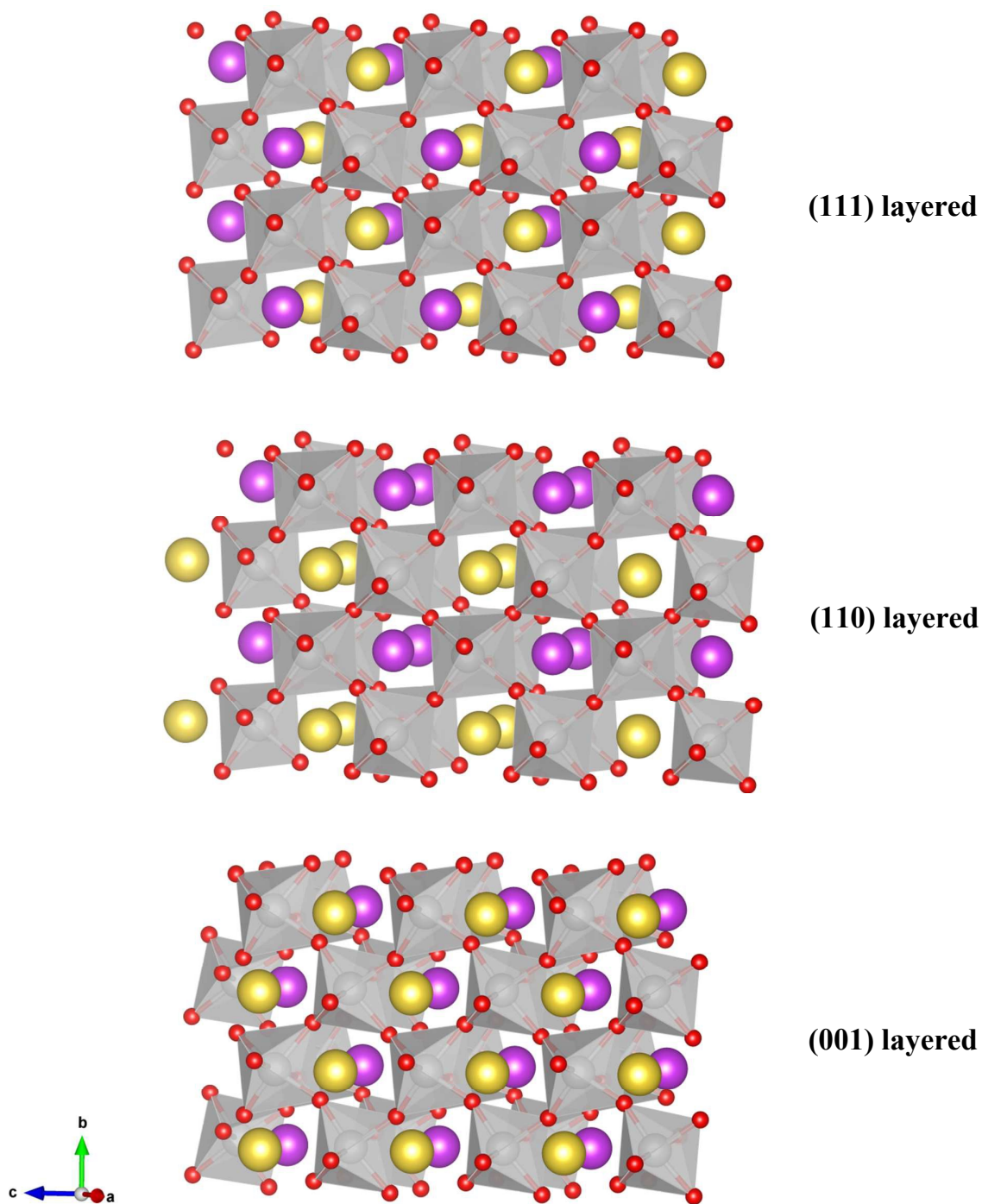


Fig. 1. Optimized NBT Cc supercells. Na ions are represented by yellow spheres, Bi ions are purple, Ti ions are silver and oxygen ions are red.

Table 1. Calculated lattice parameters and relative stabilities for the NBT *Cc* unit cell structures.

Structure	<i>a</i> (Å)	<i>b</i> (Å)	<i>c</i> (Å)	Angle (β) (deg)	Relative stability (eV/f.u.)
(111) layered	9.67	5.48	5.57	125.18	+0.06
(110) layered	9.60	5.56	5.63	125.27	+0.04
(001) layered	9.60	5.55	5.61	124.84	0
Experiment ¹⁶	9.53	5.48	5.51	125.34	-

The lattice parameters and relative stabilities of the *R3c* configurations are given in Table 2. Again a slight overestimation of the lattice parameters is observed, but the values are still mostly well within 2% of the experimental values. As was the case for the *Cc* structure, the lowest energy found was for (001) layered ordering. The energy difference between the three structures is again minute and indeed smaller than the difference seen for the *Cc* structure which suggests that the stabilizing effect of the layered structure is marginally greater for *Cc* than for *R3c*. The relative energies for all configurations tested are plotted in Figure 2. Each respective *Cc* structure is slightly more stable than its *R3c* equivalent. The total energy difference between the most and least stable configurations is only 0.07 eV per formula unit. These results strongly support the existence of a random distribution of A-site ions in NBT.

Table 2. Calculated lattice parameters and relative stabilities for the two most stable NBT $R3c$ unit cell structures.

Structure	a (Å)	b (Å)	c (Å)	Relative stability (eV/f.u.)
(111) layered	5.55	5.55	13.80	+0.04
(110) layered	5.55	5.55	13.79	+0.02
(001) layered	5.56	5.56	13.65	0
Experiment ¹⁵	5.49	5.49	13.51	-

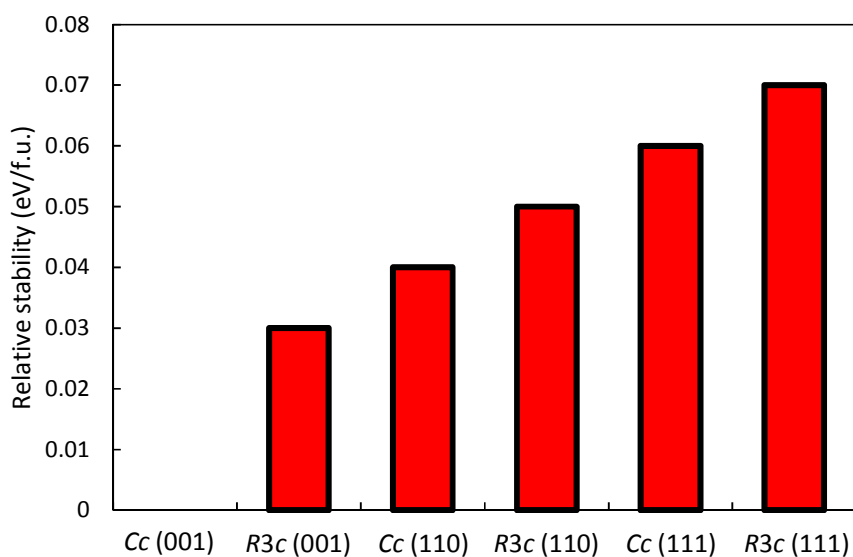


Fig. 2. Relative stabilities of the lowest energy NBT Cc and $R3c$ unit cell structures.

Previous DFT calculations²⁰ have suggested that the stabilization of the (001) layered structure in NBT arises from oxygen ions being displaced towards stronger bonding Bi ions. The proposed reason for this is because in the (001) layered structure, two thirds of the oxygen ions are in cis coordination (see Fig. 3) with regard to the surrounding A-site ions, meaning the oxygen ions can be displaced more easily. This phenomenon was not observed

for any of the NBT configurations considered in this earlier work. This is somewhat surprising given that the (110) configuration also has two thirds of its oxygen ions in the same coordination, yet it receives no such stability gain. It is also surprising that the formation of strong Bi-O bonds is proposed as the mechanism for stabilizing the (001) structure as experiment has proposed that weak Bi-O bonds with varying lengths are common in non-cubic polytypes^{35,36} and may be the reason for the unusual levels of oxygen migration in this material¹¹. Furthermore, no displacements on the two cation sub-lattices, in direct contradiction to this work and several experimental studies^{11,14,18}. This is likely a result of the fact that Gröting *et al.*²⁰ considered only ideal, small cubic supercells. Our calculations show that the average Bi-O and Na-O distances are both important in determining the stability ordering in NBT.

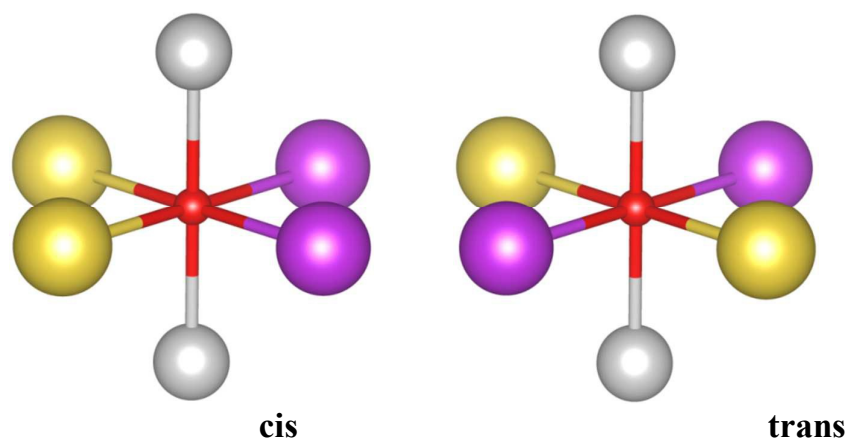


Fig. 3. Illustration of the cis and trans 2 X Bi/2 X Na oxygen environments in the NBT structure.

As the bonding in the *Cc* and *R3c* structures is almost identical, the following discussion applies for both structures. We analysed all the local oxygen bonding environments for every structure and in agreement with experiment³⁷, observed significant oxygen displacement in all the configurations, however, no strong evidence of overall oxygen displacement towards

only the Bi or Na ions. Such oxygen displacement is just the result of local disorder and heavily tilted TiO_6 octahedra. Moreover, the smallest Bi-O bonds (2.31 and 3.32 Å) were found in the higher energy (110) layered structures, thus suggesting that there must be other factors involved in the stabilization of the (001) structure other than the formation of unusually small Bi-O bonds. The strength of the Bi-O interactions in NBT is a topic that we return to in our discussion of oxygen vacancies (section 3.2). The unbiased nature of oxygen displacements is clearly illustrated by the two cis oxygen bonding environments in the (001) layered structure shown in Fig. 4. In environment 1, a very short Na-O bond and a very long Bi-O bond are formed which suggests oxygen displacement towards the Na ions, whereas in environment 2 two shorter Bi-O bonds and one long Na-O bond are formed which suggests displacement towards the Bi ions.

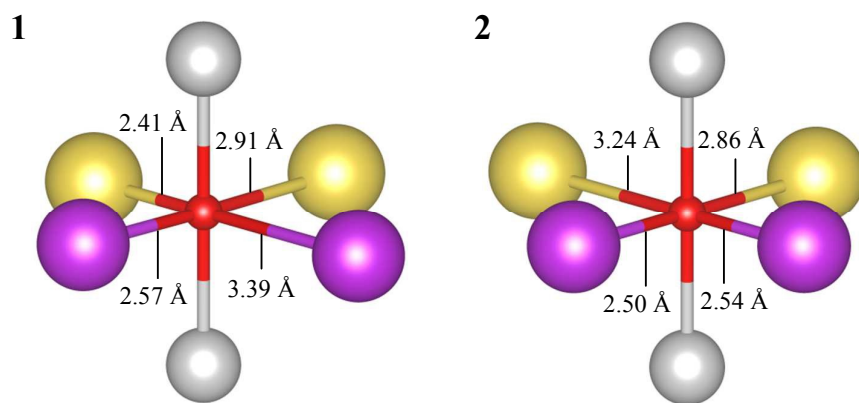


Fig. 4. Illustration of the two cis 2 X Bi/2 X Na oxygen environments in the (001) layered NBT structure.

Table 3 shows the calculated average Bi-O, Na-O and overall A-O bond lengths in each of the three NBT configurations considered. All the average bond lengths are very similar,

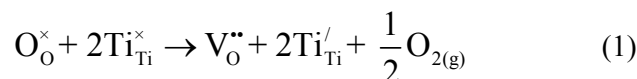
which is in agreement with our observation that oxygen displacement is strongly favoured towards neither Bi nor Na ions. However, it should be noted that the average Bi-O bond length in the (110) and (001) structures, which have the cis/trans 2 X Bi/2 X Na oxygen environments, is marginally shorter than in the rock salt structure, perhaps suggesting a very modest preference for oxygen displacement towards the Bi ions in these structures. The similar average A-O bond lengths are also in agreement with the small differences in stability between these structures. The (001) layered structure has the lowest average Bi-O and Na-O bond lengths which explains why it is the most stable out of the three structures. The (111) and (110) layered structures have the same average A-O bond length, however, in the (110) structure, the average Bi-O bond length is smaller which may explain why (110) is more stable than (111). Although the average bond lengths for all three structures are alike, the deviation is large with Bi-O bonds ranging from 2.31 to 3.39 Å and Na-O bonds between 2.38 and 3.24 Å.

Table 3. Average A-O bond distances for each of the NBT configurations.

Configuration	Average Bi-O bond length (Å)	Average Na-O bond length (Å)	Average A-O bond length (Å)
(111) layered	2.82	2.82	2.82
(110) layered	2.81	2.83	2.82
(001) layered	2.79	2.80	2.80

3.2. Oxygen Vacancy Formation in NBT

Oxygen vacancy formation energies in this work are calculated from the following reduction reaction:

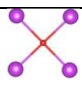
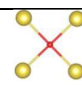
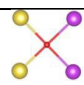
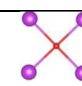
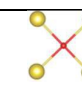
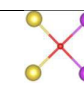


i.e. one oxygen vacancy per 120 atom NBT supercell. In all our calculations, the supercell is neutral with the electronic charge around the vacancy self-consistently redistributed. We therefore assume a reduction cluster where two reduced Ti ions neighbour the oxygen vacancy. A similar approach was taken in our recent works on $\beta\text{-MnO}_2$ ^{38,39}. In order to calculate the defect formation energy of an oxygen vacancy, the energy of a reference isolated spin triplet oxygen molecule must also be calculated. This is achieved by simulating the oxygen molecule in a large cubic cell using the same calculation conditions used for the NBT calculations. We obtain an energy of -9.09 eV for the oxygen molecule.

We begin by discussing the results for the (001) layered structure as this structure contains three distinct oxygen bonding environments: 4 X Bi, 4 X Na and 2 X Bi/2 X Na (cis). This allows us to assess the individual contribution from the Bi and Na ions on the stability and strength of each particular bonding environment. The oxygen vacancy formation energies for the (001) layered structure are given in Table 4. Vacancy formation energies for the *Cc* and *R3c* structures are very similar with slight variations coming from the difference between the supercell shapes and volumes. The lowest formation energies are observed for oxygen vacancies formed in the 4 X Bi coordination, while the highest formation energies are for oxygen vacancies formed in the 4 X Na coordination. This is contrary to simple Coulombic arguments where higher charged Bi^{3+} cations would be expected to form stronger bonds to the oxygen ions compared to the Na^{+} cations. It is, however, in complete agreement with

experimental hypotheses of weak Bi-O bonds in NBT and that off-centring and the high polarizability of Bi ions may be a crucial factor in the unusual high oxygen ion conductivity in this material. These results suggest a greater concentration of oxygen vacancies in Bi-rich structural environments and therefore an enhancement in oxygen ion conductivity.

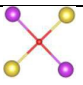
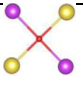
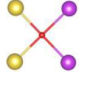
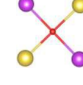
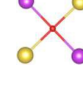
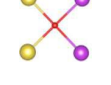
Table 4: Lowest oxygen vacancy formation energies based on Equation 1 for each A-O coordination in the (001) NBT structures.

A-O coordination	ΔE_F (eV)
<i>Cc</i> 4 X Bi 	4.71
<i>Cc</i> 4 X Na 	5.62
<i>Cc</i> 2 X Bi/2 X Na (cis) 	5.26
<i>R3c</i> 4 X Bi 	4.72
<i>R3c</i> 4 X Na 	5.62
<i>R3c</i> 2 X Bi/2 X Na (cis) 	5.31

The lowest oxygen vacancy formation energies for the (110) and (111) structures are given in Table 5. For the (110) structures, the lowest oxygen vacancy formation energies are calculated for the cis configurations, this is again a result of weak Bi-O bonding. Fig. 5 shows three *R3c* (110) oxygen configurations, for the cis configuration with the short Bi-O bonds, the vacancy energy is at a minimum, whereas for the cis configuration with the long Bi-O

bonds, the vacancy energy is at a maximum. In agreement with the results for the (001) structures, this clearly demonstrates how Bi ions actively promote the creation of oxygen vacancies and that the Na-O bonds in NBT are significantly stronger than the Bi-O bonds. As there are two Bi ions in each of these configurations, the lowest vacancy formation energy is still not as low as for the (001) 4 X Bi configuration. For the (110) trans configuration, the formation energy is in between the minimum and maximum values for the cis configurations, as neither short Bi-O or short Na-O bonds can form (Fig. 5). There is only possible configuration for the (111) structures and therefore there is little variation in oxygen vacancy formation energy and the values are similar to the equivalent configuration in the (110) structure.

Table 5: Lowest oxygen vacancy formation energies based on Equation 1 for each A-O coordination in the (111) and (110) NBT structures.

A-O coordination	ΔE_F (eV)
<i>Cc</i> (111) 2 X Bi/2 X Na (trans) 	4.97
<i>Cc</i> (110) 2 X Bi/2 X Na (trans) 	5.01
<i>Cc</i> (110) 2 X Bi/2 X Na (cis) 	4.93
<i>R3c</i> (111) 2 X Bi/2 X Na (trans) 	4.92
<i>R3c</i> (110) 2 X Bi/2 X Na (trans) 	4.94
<i>R3c</i> (110) 2 X Bi/2 X Na (cis) 	4.85

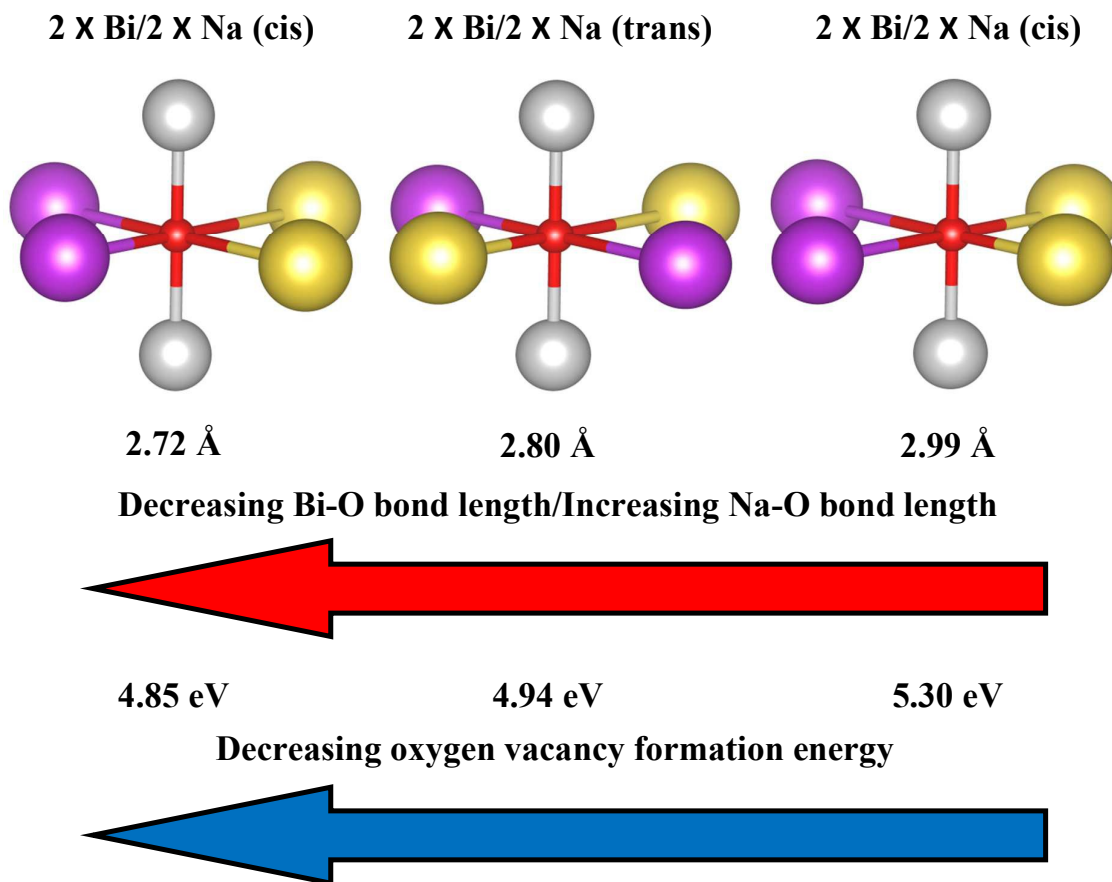


Fig. 5. Illustration of three different oxygen bonding environments in the NBT $R3c$ (110) structure and the effect Bi-O bond length has on the oxygen vacancy formation energy.

As the discovery of high levels of oxygen ion conductivity in NBT is very recent, there is very little experimental or computational work on oxygen vacancies to compare our results to. One exception to this is a DFT study of cation and oxygen vacancies in NBT by Zhang et al.⁴⁰. In this study, a value of 4.37 eV was calculated for an oxygen vacancy in the rhombohedral $R3c$ structure, however comparison is difficult as it is unclear whether this was oxygen was taken from a cis/trans or Ni/Bi-rich environment. Regardless, their value is lower than any of our oxygen vacancy formation energies, this is likely a result of the small

supercell and different computational parameters (e.g. larger value of U for the Dudarev correction) used in the previous study. The same authors also calculated vacancy formation energies for each cation species. As expected, the Ti vacancy was highest in energy (17.75 eV). Interestingly, the energy for a Bi vacancy (8.14 eV) was found to be significantly lower than that for a Na vacancy (12.82 eV), this is in complete agreement with our results which suggest weak Bi-O interactions and stronger Na-O interactions.

There is also information in the literature available on oxygen vacancy formation in other titanate perovskites and perovskite oxygen ion conductors. Our calculated value of 4.71 eV for oxygen vacancy formation in the NBT Cc (001) structure is lower than the equivalent values calculated for titanates including $BaTiO_3$ ^{41,42}, $SrTiO_3$ ⁴³ and $PbTiO_3$ ⁴⁴. This further illustrates the contribution of Bi ions to some of the unusually low oxygen vacancy formation energies in NBT. However, these low formation energies are still significantly higher those observed for non-titanate perovskite oxygen ion conductors like $(La,Sr)(Fe,Co)O_{3-\delta}$ and $(Ba,Sr)(Fe,Co)O_{3-\delta}$ (~1.5 to 4.5 eV)⁴⁵.

3.3. Oxygen migration in NBT

Given that the (001) layered structure possesses three distinct oxygen coordination environments and that the oxygen vacancy formation energies between the Cc and $R3c$ structures are very similar, we focus on the Cc (001) structure for the calculation of oxygen migration energies. We consider all five possible pathways: from the mixed A-site layer to the Bi layer and vice versa, from the mixed A-site layer to the Na layer and vice versa and migration between oxygen vacancies in the mixed A-site layer. These pathways are illustrated for a simple NBT cubic unit cell in Figure 6. Oxygen ion pairs with the shortest interatomic distance between are chosen for the migration pathways. Therefore, our reported

migration energies are highly likely to reflect the lowest possible energy pathways in this structure. By testing these five unique pathways, we can fully determine the contribution of each oxygen coordination environment to the migration energetics and answer the question of whether Bi ions are indeed a primary factor in the conduction behaviour of NBT. To the best of our knowledge, this is the first time that oxygen migration has been studied in such detail and migration energies have been calculated.

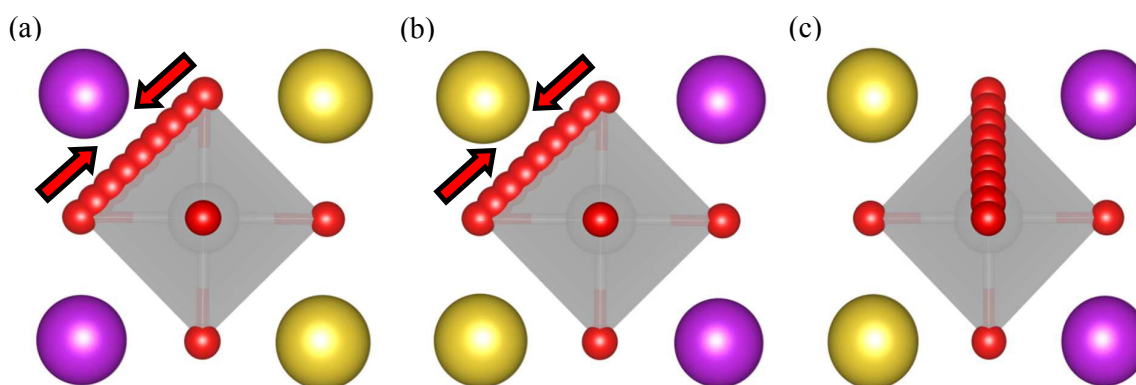


Fig. 6. Illustrations displaying the five oxygen migration pathways for the NBT Cc (001) layered structure. (a) Migration from the mixed A-site layer to the Bi layer and vice versa, (b) migration from the mixed A-site layer to the Na layer and vice versa and (c) migration within the mixed A-site layer.

Energy profiles for the five oxygen migration pathways in NBT Cc (001) structure are displayed in Figure 7. The migration barriers range from 0.56 to 0.85 eV with oxygen migration from the mixed A-site layer to the Na layer being the lowest in energy and migration from the mixed A-site layer to the Bi layer having the highest. Two of the important factors that determine the migration energy barrier are the nature of the A-site ions in the “critical triangle” that the oxygen passes through and the nature of the location where the oxygen is moving to. For example, for migration to the Bi layer, the critical triangle

contains two Bi ions and we have already shown that bonding between Bi and oxygen ions is weak in NBT. Furthermore, the oxygen is also moving to a less stable site as a result of this weak bonding in the Bi layer and as a result the migration barrier is high (0.85 eV). Conversely, when the critical triangle contains two more favourable Na ions and the oxygen ion is moving to the Na layer, the migration barrier is at a minimum (0.56 eV).

This is further illustrated by the migration pathways from the Bi and Na layers to the mixed A-site layer. In the case of migration from the Bi layer to the mixed layer, although the critical triangle contains unfavourable Bi ions, the oxygen is migrating from the unfavourable Bi layer and closer towards the Na layer and therefore the migration energy is low (0.63 eV). The opposite is true for migration from the Na layer where the critical triangle is favourable, but the oxygen must overcome the stronger bonding of the Na ions and therefore the migration barrier is higher (0.77 eV). Similar results were recently found for $\text{La}_{0.5}\text{Sr}_{0.5}\text{FeO}_{3-\delta}$ ⁴⁵, it was discovered that critical triangles containing one or two Sr ions (as opposed to La ions) produced higher migration barriers because of the weaker attraction between them and the migrating oxygen compared. The influence of A-site charge/size on migration barriers has also been confirmed for LaGaO_3 ⁴⁶. The barrier for migration within the mixed layer is 0.71 eV and can be considered an average of the other energies as it neither gains the energetic benefit of moving towards the Na layer or the energetic penalty of moving towards the Bi layer.

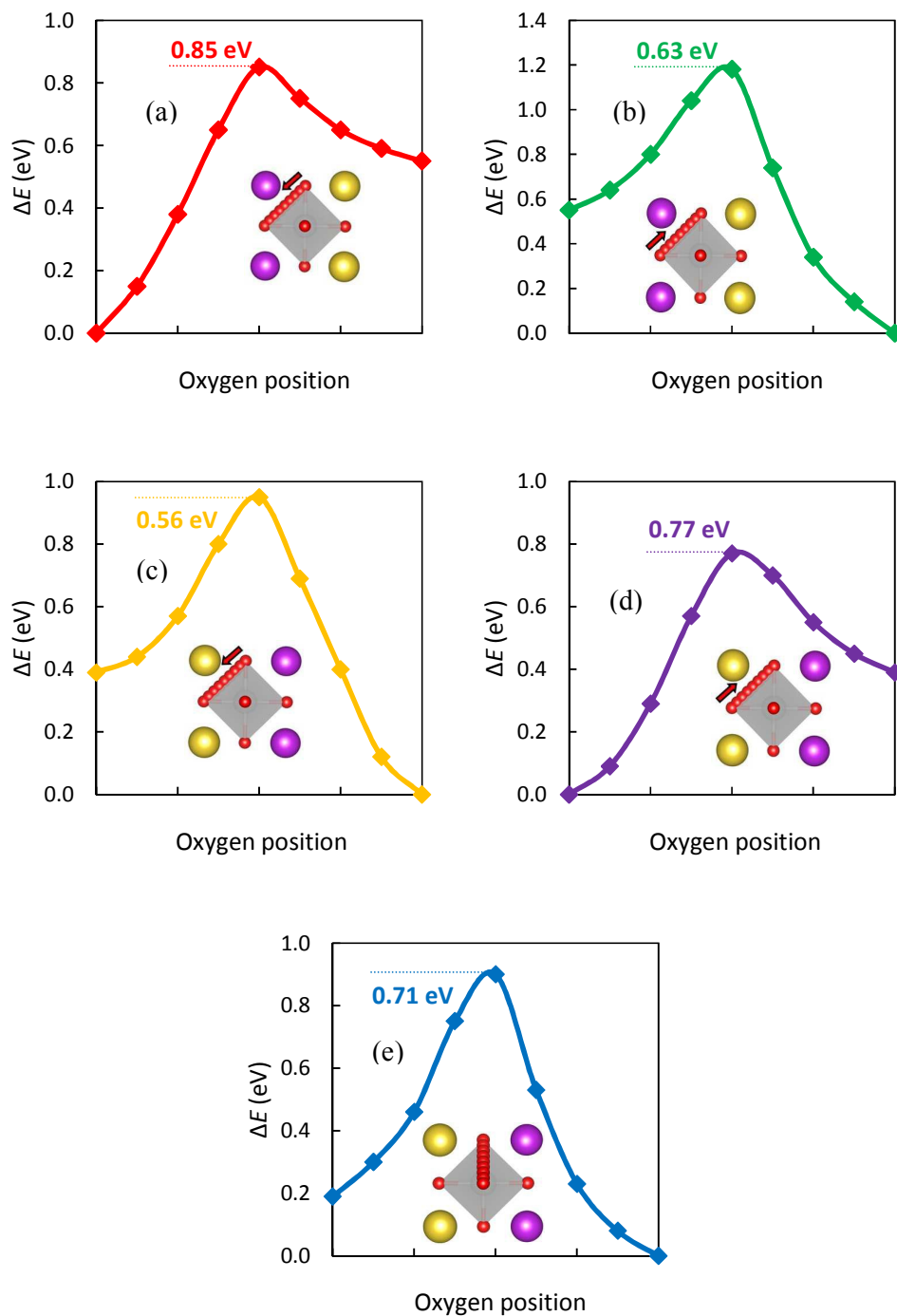


Fig. 7. Energetics for oxygen migration in the the NBT Cc (001) layered structure. (a) Migration from the mixed A-site layer to the Bi layer, (b) migration from the Bi layer to the mixed A-site layer, (c) migration from the B-site layer to the Na layer, (d) migration from the Na layer to the mixed A-site layer and (e) migration within the mixed A-site layer.

In addition to discussing the migration barriers in isolation, they must also be considered in the context of oxygen vacancy stability. Our results have shown that the highest concentration of oxygen vacancies is likely to be in Bi-rich environments and therefore migration to the Bi layer is likely to be an important pathway, even though this pathway has the highest migration energy. Likewise, while migration towards Na ions may be the most energetically favoured pathway, there is likely to be far less oxygen vacancies in the Na layer. This is a point that warrants further investigation, possibly using kinetic Monte Carlo or molecular dynamics simulations. Based on our results, the answer to whether Bi ions do promote oxygen ion conductivity in NBT is yes, however it is perhaps not as simple as it first appears. Weak Bi-O bonds certainly promote oxygen vacancies and any oxygen migration from away Bi ions is energetically very favourable. However, as we have discussed, oxygen migration to the oxygen vacancy rich Bi layers is unfavourable, although the energy is by no means too high to be considered a detriment to oxygen transport.

Impedance spectroscopy and ^{18}O tracer diffusion measurements¹¹ have been used to identify oxygen ion conduction activation energies of 0.8-0.9 eV and 0.4-0.5 eV for temperature ranges below and above 320 °C in NBT. Generally, our values are in between these two sets of energies, however it is very interesting that our value for migration to the Bi layer (0.85 eV) is in excellent agreement with the experimental activation energy for temperatures below 320 °C. Our calculated values are also very comparable with migration barriers for well-known perovskite oxygen conductors such as $\text{La}_{1-x}\text{Sr}_x\text{Co}_{1-y}\text{Fe}_y\text{O}_{3-\delta}$ and $\text{Ba}_{1-x}\text{Sr}_x\text{Co}_{1-y}\text{Fe}_y\text{O}_{3-\delta}$ ^{45,47}. Mg-doping has already been shown to dramatically increase the ionic conductivity of NBT¹¹, we hope to assess the effects of Mg and other dopant ions on oxygen migration in a future study. Through tailoring and optimizing the A-/B-site dopant structure, experimentally and computationally, the true potential of this unique material can be achieved.

4. Conclusions

In this work, through the use of DFT calculations, we have clearly demonstrated the particular importance of Bi in determining the unique defect chemistry and potential role of NBT as an oxygen ion conductor for application in intermediate-temperature SOFCs. We have analysed local A-site ordering in both of the proposed room temperature structures (*Cc* and *R3c*), calculated oxygen vacancy formation energies for all oxygen ions in a variety of configurations and structures and determined the likely oxygen migration pathways in the material.

Our calculations have revealed that although there is an energetic preference for A-site (001) layered ordering, the energy difference between the least and most stable of all *Cc* and *R3c* configurations tested is only 0.07 eV per formula unit, thus supporting the experimental observation of a random distribution of A-site ions in NBT. The stabilization of the (001) layering was found to be primarily the result of marginally lower average A-O bond lengths compared to other orderings. We calculated low oxygen vacancy formation energies of 4.71 and 4.72 eV for oxygen ions in Bi-rich coordination and reduced formation energies were found for local configurations with short Bi-O bond lengths. These results clearly illustrate the weak Bi-O bonding in NBT and more importantly, how these bonds promote the formation of oxygen vacancies, thus increasing oxygen ion conduction. Oxygen migration barriers calculated for the (001) structure range from 0.56 to 0.85 eV, in excellent agreement with experiment. Migration from the mixed A-site layer to the Na layer is the lowest in energy and migration from the mixed A-site layer to the Bi layer is the highest. We have shown how both the constituents of the migration “critical triangle” and the stability of the start and end site of the migration pathway are crucial to determining the migration energy.

We hope that the results and ideas presented in this study can be applied to maximise oxygen ion conduction in this exciting material and assist in its possible application in fuel cell electrolytes/electrodes.

ACKNOWLEDGEMENTS

The authors thank the Japan Society for the Promotion of Science (JSPS) for funding through Grants-in-Aid for (a) Scientific Research on Innovative Areas "Nano Informatics" (Grant No. 25106005) and for (b) JSPS fellows (Grant No. 2503370).

REFERENCES

- (1) Saito, Y.; Takao, H.; Tani, T.; Nonoyama, T.; Takatori, K.; Homma, T.; Nagaya, T.; Nakamura, M. *Nature*, **2004**, *432*, 84.
- (2) Shrout, T. R.; Zhang, S. J. *J. Electroceram.* **2007**, *19*, 113.
- (3) Rodel, J.; Jo, W.; Seifert, K. T. P.; Anton, E. M.; Granzow, T.; Damjanovic, D. *J. Am. Ceram. Soc.* **2009**, *92*, 1153.
- (4) Park, S.-E.; Chung, S.-J.; Kim, I.-T. *J. Am. Ceram. Soc.* **1996**, *79*, 1290.
- (5) Hiruma, Y.; Nagata, T.; Takenaka, T. *J. Appl. Phys.* **2009**, *105*, 084112.
- (6) Guo, Y.; Liu, Y.; Withers, R. L.; Brink, F.; Chen, H. *Chem. Mater.* **2011**, *23*, 219.
- (7) Dittmer, R.; Jo, W.; Roedel, J.; Kalinin, S.; Balke, N. *Adv. Funct. Mater.* **2012**, *22*, 4208.
- (8) Wang, X. X.; Tang, X. G.; Chan, H. L. W. *Appl. Phys. Lett.* **2004**, *85*, 91.
- (9) Chiang, Y. M.; Farrey, G. W.; Soukhojak, A. N. *Appl. Phys. Lett.* **1998**, *73*, 3683.

- (10) Patterson, E. A.; Cann, D. P.; Pokorny, J.; Reaney, I. M. *J. Appl. Phys.* **2012**, *111*, 094105.
- (11) Li, M.; Pietrowski, M. J.; De Souza, R. A.; Zhang, H.; Reaney, I. M.; Cook, S. N.; Kilner, J. A.; Sinclair, D. C. *Nat. Mater.* **2014**, *13*, 31.
- (12) Li, M.; Zhang, H.; Cook, S. N.; Li, L.; Kilner, J. A.; Reaney, I. M.; Sinclair, D. C. *Chem. Mater.* **2015**, *27*, 629.
- (13) Smolenskii, G. A.; Isupov, V. A.; Agranovskaya, A. I.; Popov, S. N. *Phys. Solid State* **1961**, *2*, 2584.
- (14) Levin, I.; Reaney, I. M. *Adv. Funct. Mater.* **2012**, *22*, 3445.
- (15) Jones, G. O.; Thomas, P. A. *Acta Crystallogr., Sect. B: Struct. Sci.* **2002**, *58*, 168.
- (16) Aksel, E.; Forrester, J. S.; Jones, J. L.; Thomas, P. A.; Page, K.; Suchomel, M. R. *Appl. Phys. Lett.* **2011**, *98*, 152901.
- (17) Keeble, D. S.; Barney, E. R.; Keen, D. A.; Tucker, M. G.; Kreisel, J.; Thomas, P. A. *Adv. Funct. Mater.* **2012**, *23*, 185.
- (18) Aksel, E.; Forrester, J. S.; Nino, J. C.; Page, K.; Shoemaker, D. P.; Jones, J. L. *Phys. Rev. B* **2013**, *87*, 104113.
- (19) Kreisel, J.; Bouvier, P.; Dkhil, B.; Thomas, P. A.; Glazer, A. M.; Welberry, T. R.; Chaabane, B.; Mezouar, M. *Phys. Rev. B* **2003**, *68*, 014113.
- (20) Gröting, M.; Hayn, S.; Albe, K. *J. Solid State Chem.* **2011**, *184*, 2041.
- (21) Sung, Y. S.; Kim, J. M.; Cho, J. H.; Song, T. K.; Kim, M. H.; Park, T. G. *Appl. Phys. Lett.* **2011**, *98*, 012902.
- (22) Spreitzer, M.; Valant, M.; Suvorov, D. *J. Mater. Chem.* **2007**, *17*, 185.
- (23) Zeng, M.; Or, S. W.; Chan, H. L. W. *J. Appl. Phys.* **2010**, *107*, 043513.
- (24) Carter, J.; Aksel, E.; Iamsasri, T.; Forrester, J. S.; Chen, J.; Jones, J. L. *Appl. Phys. Lett.* **2014**, *104*, 112904.

- (25) Kresse, G.; Furthmüller, J. *Comput. Mater. Sci.* **1996**, *6*, 15.
- (26) Perdew, J. P.; Burke, K.; Ernzerhof, M. *Phys. Rev. Lett.* **1996**, *77*, 3865.
- (27) Blöchl, P. E. *Phys. Rev. B* **1994**, *50*, 17953.
- (28) Dudarev, S. L.; Botton, G. A.; Savrasov, S. Y.; Humphreys, C. J.; Sutton, A. P. *Phys. Rev. B* **1998**, *57*, 1505.
- (29) Morgan, B. J.; Watson, G. W. *Surf. Sci.* **2007**, *601*, 5034.
- (30) Morgan, B. J.; Watson, G. W. *Phys. Rev. B* **2010**, *82*, 144119.
- (31) Kilner, A.; Brook, R. J.; *Solid State Ionics* **1982**, *6*, 237.
- (32) Cherry, M.; Islam, M. S.; Catlow, C. R. A. *J. Solid State Chem.* **1995**, *118*, 125.
- (33) Dorcet, V.; Trolliard, G.; Boullay, P. *Chem. Mater.* **2008**, *20*, 5061.
- (34) Gröting, M.; Kornev, I.; Dkhil, B.; Albe, K. *Phys. Rev. B* **2012**, *86*, 134118.
- (35) Schütz, D.; Deluca, M.; Krauss, W.; Feteira, A.; Jackson, T.; Reichmann, K. *Adv. Funct. Mater.* **2012**, *22*, 2285.
- (36) Keeble, D. S.; Barney, E. R.; Keen, D. A.; Tucker, M. G.; Kreisel, J.; Thomas, P. A. *Adv. Funct. Mater.* **2012**, *23*, 185.
- (37) King, G.; Woodward, P. M. *J. Mater. Chem.* **2010**, *20*, 5785.
- (38) Dawson, J. A.; Tanaka, I. *ACS Appl. Mater. Interfaces* **2014**, *6*, 17776.
- (39) Dawson, J. A.; Chen, H.; Tanaka, I. *ACS Appl. Mater. Interfaces* **2015**, *7*, 1726.
- (40) Zhang, Y.; Hu, J.; Gao, F.; Liu, H.; Qin, H. *Comp. Theor. Chem.* **2011**, *967*, 284.
- (41) Erhart, P.; Albe, K. *J. Appl. Phys.* **2007**, *102*, 084111.
- (42) Dawson, J. A.; Harding, J. H.; Chen, H.; Sinclair, D. C. *J. Appl. Phys.* **2012**, *111*, 094108.
- (43) Dawson, J. A.; Chen, H.; Tanaka, I. *J. Phys. Chem. C* **2014**, *118*, 14485.
- (44) Zhang, Z.; Wu, P.; Lu, L.; Shu, C. *J. Alloy Compd.* **2008**, *449*, 352.

- (45) Mastrikov, Y. A.; Merkle, R.; Kotomin, E. A.; Kuklja, M. M.; Maier, J. *Phys. Chem. Chem. Phys.* **2013**, *15*, 911.
- (46) De Souza, R. A.; Martin, M. *Monasth. Chem.* **2009**, *140*, 1011.
- (47) Chroneos, A.; Yildiz, B.; Tarancon, A.; Parfitt, D.; Kilner, J. A. *Energy Environ. Sci.* **2011**, *4*, 2774.

TOC

